2025 IMEKO TC26 International Conference on
Metrology for Archaeology and Cultural Heritage
Bergamo, Italy, October 15-17, 2025

Natural radioactivity content, radiological hazard and mineralogy evaluation of *Pumice* stone from Lipari, Sicily, Southern Italy: a case study

Lorenzo Pistorino[1]*, Francesco Caridi[1]*, Giuseppe Paladini[1], Antonio Francesco Mottese[2]
Domenico Majolino[1], Valentina Venuti[1]

[1] *Dipartimento di Scienze Matematiche e Informatiche, Scienze Fisiche e Scienze della Terra, Università degli Studi di Messina, V.le F. Stagno D'Alcontres, 31-98166 Messina, Italy, lorenzo.pistorino@studenti.unime.it (*corresponding author), fcaridi@unime.it (*corresponding author), gpaladini@unime.it, dmajolino@unime.it, vvenuti@unime.it*
[2]*Dipartimento di Ingegneria dell'Informazione, delle Infrastrutture e dell'Energia Sostenibile (DIIES), Università "Mediterranea", Via Zehender, 89122 Reggio Calabria, Italy, antonio.mottese@unirc.it*

***Abstract* – In this paper, an assessment of natural radioactivity content, radiological hazard for human beings and mineralogical composition of a pumice rock sample from Lipari Island (Sicily, Southern Italy), historically employed as a building material, is presented as a case study.**
The specific activity of ^{226}Ra, ^{232}Th, and ^{40}K was assessed by means of High-Purity germanium (HPGe) gamma-ray spectrometry. Based on the obtained data, several indices were calculated – namely the absorbed dose rate (D), the Annual Effective Dose Equivalent (AEDE), the Activity Concentration Index (I_γ) and the alpha index (I_α) – in order to estimate potential radiological hazards from prolonged exposure to ionizing radiation. As a result, while I_α remains below the recommended threshold, the remaining radiological health hazard indices exceed internationally recognized safety limits, suggesting potential implications for the use of Lipari pumice in construction applications.
Furthermore, with the aim of identifying the radioisotope-bearing mineral phases within the pumice matrix, X-Ray Fluorescence (XRF) spectroscopy and X-Ray Diffraction (XRD) measurements were carried out. The results of this study offer a valuable reference for future investigations on background radioactivity levels in natural stones commonly employed as building materials. Notably, given the lack of prior studies on the radiological impact of Lipari pumice, this work represents a novel contribution to the field, offering new insights into its radioactive properties.

I. INTRODUCTION

Human exposure to ionizing radiation arises from both natural, i.e. primordial and cosmogenic radionuclides, and artificial sources [1]. Primordial radionuclides - including the decay series of ^{238}U, ^{232}Th, and ^{235}U - are ubiquitously present in the Earth's crust since its formation. In particular, their concentration depends on local geology, mineral composition, and tectonic history, resulting in spatial variations in terrestrial radiation levels worldwide. On the other hand, human exposure to cosmogenic radionuclides varies with factors such as altitude, geographic location, and atmospheric conditions, which affect cosmic radiation intensity and isotope formation.

Conversely, artificial radioactivity is due to radionuclides (e.g. ^{239}Pu, ^{137}Cs, ^{131}I) mainly derived from human activities, including nuclear accidents, nuclear power generation, medical applications, and industrial processes.

Going on, among the key contributors to indoor radiation exposure there are natural stone materials, frequently employed as building materials. Given their widespread use in construction - ranging from structural components to decorative elements - in recent years the radioactivity content of these materials became a key focus of extensive research activities [2]. This growing international interest stems from the fact that naturally occurring radionuclides (NORMs) in building materials pose two primary exposure risks: external exposure, due to gamma radiation emission, and internal exposure, resulting from the inhalation of radon (^{222}Rn) and its short-lived alpha progeny ^{218}Po and ^{214}Po.

In this paper, a multi-technique investigation was carried out in order to evaluate both the radioactivity content and the elemental and mineralogical composition of a pumice rock sample from Lipari Island (Sicily, Southern Italy). In particular, High-Purity Germanium (HPGe) gamma-ray spectrometry measurements were performed to investigate the activity concentrations of natural radionuclides (i.e.

^{226}Ra, ^{232}Th and ^{40}K). Then, several radiological indices - including the absorbed gamma dose rate (D), the Annual Effective Dose Equivalent (AEDE), the activity concentration index (I_γ) and the alpha index (I_α) - were calculated to evaluate the potential radiological hazard for humans associated with long-term exposure to the investigated material. Thereafter, complementary elementary and mineralogical investigations were carried out by means of X-Ray Fluorescence (XRF) spectroscopy and X-Ray Diffraction (XRD), aimed at identifying the specific radioisotope-bearing phases within the pumice matrix.

It is worth noting that Lipari pumice has long been used in construction - especially for lightweight concrete, paving, and architectural slabs - due to its excellent physical and mechanical properties [3]. Therefore, given the extensive historical use of this volcanic stone as building material, a thorough evaluation of its radioactivity content is crucial for assessing its suitability in both current and future applications.

II. MATERIALS AND METHODS

A. Sampling

The pumice sample was collected from a now-closed quarry along Provincial Road No. 180, connecting Canneto to Porticello. Following standard sampling protocols [4], five aliquots of the analyzed stone were carefully placed in a labelled plastic container to prevent contamination. The sampling site's GPS coordinates are 38°30'35.1" N, 14°57'43.4" E (Figure 1).

Fig. 1. Geographic location of Lipari Island within the Aeolian Archipelago, in the southern Tyrrhenian Sea, north of Sicily (Italy). The main image highlights the position of Lipari Island relative to Sicily, while the inset maps show (top right) the broader location within Italy and (bottom left) a close-up view of Lipari Island with the sampling site.

B. HPGe gamma spectrometry

Prior to HPGe gamma spectrometry measurements, each aliquot was oven-dried at 105 °C, followed by grinding in a vibratory micro mill to achieve a homogeneous fine powder. The powdered material was then sieved to ensure a particle size of less than 2 mm before being placed into a hermetically sealed 250 mL Marinelli container. To enable for the establishment of secular equilibrium between ^{226}Ra and its short-lived progeny, each aliquot was stored for 30 days prior to measurement. Spectral acquisition was carried out for 70000 s, and radionuclide specific activities were determined based on their characteristic gamma-ray emissions. Specifically, ^{226}Ra activity concentration was assessed through the 295.21 keV and 351.92 keV lines of ^{214}Pb, as well as the 1120.29 keV γ-ray from ^{214}Bi. The γ-ray lines of ^{228}Ac (i.e. 911.21 keV and 968.97 keV) were used to evaluated the ^{232}Th activity concentration. Finally, the ^{40}K activity concentration was calculated from the detection of its distinctive γ-ray line at 1460.8 keV [5].

Gamma spectrometry analyses were carried out by means of an electrically cooled, direct biased HPGe GEM detector from Ortec (Oak Ridge, TN, USA), positioned within lead shielding to minimize background radiation interference. The HPGe detector is characterized by a full width at half maximum (FWHM) of 1.85 keV, a 40% relative efficiency, and a 64:1 peak-to-Compton ratio, ensuring high spectral resolution. For efficiency and energy calibration, a traceable multi-nuclide radioactive standard (Eckert & Ziegler Nuclitec GmbH, Berlin, Germany; reference number BC4464), covering an energy range from 59.54 keV to 1836.09 keV, was used. The calibration standard was designed to replicate the exact geometry of the sample, employing an epoxy resin matrix with a water-equivalent density. Data acquisition and processing were performed using Ortec Gamma Vision software.

The activity concentration (Bq kg^{-1} dry weight, d.w.) of each detected radionuclide was calculated using the following equation [6]:

$$C\ (\mathrm{Bq\ kg^{-1}}) = \frac{N_E}{\varepsilon_E t \gamma_d M} \quad (1)$$

where N_E and ε_E are the net area of the peak at energy E and the calibration efficiency at energy E, respectively, while t is the acquisition time (in s), γ_D is the branching ratio and M is the dry mass of the analyzed sample (in kg).

The high quality and reliability of the gamma spectrometry results were officially recognized by the Italian Accreditation Body (ACCREDIA).

C. Radiological Health Hazard

The radiological health hazard was initially assessed by calculating the absorbed gamma dose rate, D (nGy h^{-1}), for indoor external exposure, based on the standard room model [7]:

$$D = 0.92\ C_{Ra} + 1.1\ C_{Th} + 0.08\ C_K \quad (2)$$

where C_{Ra}, C_{Th}, and C_K are the average specific activities of ^{226}Ra, ^{232}Th, and ^{40}K, respectively, obtained from the analysis of the five aliquots.

The Annual Effective Dose Equivalent, AEDE (mSv y^{-1}) for indoor exposure was assessed by employing the following relationship [8]:

$$AEDE = (D - 50) \times 8760\ h \times 0.7\ Sv\ Gy^{-1} \times 0.8 \times 10^{-6} \quad (3)$$

in which the world average background dose rate value of 50 nGy h^{-1} was discounted, 0.7 Sv Gy^{-1} is a conversion factor and the occupancy factor 0.8 was included to take into account that people, on average, spend 80% of their time indoor. The AEDE value must remain below 1 mSv y^{-1} to guarantee a negligible radiological hazard, according to what is reported in [9].

The following equation was used to determine the Activity Concentration Index (I_γ) [10]:

$$I_\gamma = C_{Ra}/300 + C_{Th}/200 + C_K/3000 \quad (4)$$

In particular, this index serves as a preliminary screening tool to identify building materials that might present a radiological risk when incorporated into construction. Specifically, materials with $I_\gamma > 1$ should be avoided, as they correspond to dose rates exceeding 1 mSv y^{-1}, thus surpassing the recommended safety threshold.

Finally, the alpha index is used to evaluate the additional alpha radiation exposure resulting from radon inhalation originating from building materials [11]:

$$I_\alpha = C_{Ra}/200 \quad (5)$$

In detail, to ensure that indoor radon concentrations remain below the recommended reference value of 200 Bq m^{-3}, the ^{226}Ra activity concentration in building materials must not exceed 200 Bq kg^{-1}, as set by Italian Legislation [9]. Therefore, for radiation exposure to be considered negligible in terms of radiological hazard, I_α must not exceed the threshold value of 1.

D. X-Ray Fluorescence (XRF)

Elemental analysis was performed using a portable XRF analyzer (Alpha 4000, Innov-X Systems, Woburn, MA, USA), equipped with a tantalum anode X-ray tube and a silicon PIN diode detector (170 mm^2 active area, <220 eV resolution at 5.95 keV). The instrument detects elements with atomic numbers from 15 (P) to 82 (Pb).

Measurements were executed in "soil" mode, employing Compton normalization for enhanced trace element detection in the ppm range. The "Environmental" element suite included a broad range of elements (e.g., P, S, Cl, K, Ca, Fe, Pb). Each sample was analyzed through two consecutive scans (40 kV/7 μA and 15 kV/5 μA), with a total acquisition time of 120 seconds.

Data acquisition was managed via an HP iPAQ Pocket PC. Calibration was performed using the LEAP II program and verified with certified reference materials. Peaks at ~8.15 keV and ~9.34 keV correspond to the L_α and L_β emissions of the tantalum anode.

E. X-Ray Diffraction (XRD)

X-ray diffraction (XRD) analysis was performed using a Malvern PANalytical Empyrean diffractometer (Malvern, UK), equipped with a Cu K_α radiation source and a Bragg–Brentano θ-θ goniometer configuration, featuring a PIXcel solid-state detector. For each aliquot of the analyzed sample, approximately 1 gram of pumice was ground into a fine powder for the measurements. The instrument was operated at 40 kV and 40 mA. Diffraction patterns were collected over a 2θ angular range of 2° to 70°, with a step interval of 0.053° and a scan duration of 4.08 seconds per step. To correct the raw data, two separate adjustments were made: the Cu $K_{\alpha2}$ contribution was removed using HighScore Plus software (version 5.1), and background noise was minimized through digital filtering. In order to identify the mineral phases present in the powdered pumice, the positions of the observed diffraction peaks were matched against entries in the ICDD JCPDS database.

III. RESULTS AND DISCUSSION

Table 1 reports the mean activity concentrations of ^{226}Ra, ^{232}Th, and ^{40}K in the analyzed sample, calculated as the average value across five aliquots of the investigated material.

Table 1. The average ^{226}Ra, ^{232}Th and ^{40}K activity concentrations, for the analyzed natural stone.

Sample	^{226}Ra (Bq kg^{-1} d.w.)	^{232}Th (Bq kg^{-1} d.w.)	^{40}K (Bq kg^{-1} d.w.)
Lipari pumice	179 ± 21	203 ± 25	1262 ± 135

Specifically, the calculated activity concentrations markedly exceed the worldwide average levels of 35 Bq kg^{-1}, 30 Bq kg^{-1} and 400 Bq kg^{-1} for ^{226}Ra, ^{232}Th, and ^{40}K, respectively [8]. A preliminary interpretation of such elevated values can be provided widening the approach of investigation including in it also the analysis of the results of the elemental and mineralogical analyses performed, as detailed below.

To better contextualize the activity concentrations detected in Lipari pumice, Table 2 compares them with average values reported in the literature for other natural stones commonly used in construction such as red granite, basalt and tuff.

Table 2. Comparison of activity concentrations (Bq kg^{-1} dry weight) of ^{226}Ra, ^{232}Th, and ^{40}K between Lipari pumice and other natural stones commonly used in construction.

Sample	^{226}Ra (Bq kg^{-1} d.w.)	^{232}Th (Bq kg^{-1} d.w.)	^{40}K (Bq kg^{-1} d.w.)	Reference
Lipari pumice	179 ± 21	203 ± 25	1262 ± 135	This work
Red granite	20.1 ± 2.8	42.8 ± 5.9	1071 ± 127	[12]
Basalt	41.3 ± 5.1	53.1 ± 6.9	157 ± 19	[12]
Tuff	50.7	58.6	717.6	[13]

Specifically, the activity concentrations of ^{226}Ra and ^{232}Th in Lipari pumice are significantly higher than those reported for commonly used construction stones. This marked enrichment in natural radionuclides suggests a greater potential radiological impact associated with the use of Lipari pumice as a building material.

Going on, D, AEDE, I_γ and I_α, calculated according to previous equations (2) – (5), are reported in Table 3.

Table 3. The absorbed gamma dose rate (D), the Annual Effective Dose Equivalent (AEDE), the activity concentration index (I_γ) and the alpha index (I_α) for the analyzed sample.

Sample	D (nGy h^{-1})	AEDE (mSv y^{-1})	I_γ	I_α
Lipari pumice	489.1	2.2	2.0	0.9

In particular, the elevated D value - compared to the world average background of 50 nGy h^{-1} - is primarily attributable to the lithological characteristics of the sampling site [14]. It is worth noting that, although the estimated AEDE value exceeded the threshold of 1 mSv y^{-1} set by Italian legislation [9], this result was obtained under an extremely conservative scenario, assuming continuous exposure for 8760 hours per year (i.e., 24 hours a day, 365 days a year).

Moreover, an I_γ value above unity was likewise recorded, raising concerns about possible radiological effects on human health when the stone is employed in construction-related uses. These findings highlight the need for a more refined dose assessment when considering the use of natural stones in civil engineering buildings - particularly in dwellings and high-occupancy structures. Specifically, this aligns with Article 29, paragraph 5, of Italian Legislative Decree 101/2020 [9], which implements EU Directive 2013/59/Euratom [15] on basic safety standards for protection against ionising radiation. Such assessments should be carried out using nationally and internationally recognized methodologies, taking into account factors such as material density, thickness, building type and intended application. In contrast, the alpha index (I_α) was calculated to be 0.9, remaining below the critical value of 1.

Going on, Figure 2 shows the XRF spectrum of Lipari pumice natural stone, as representative of 5 different measurements collected in the energy range between 0 and 40 keV.

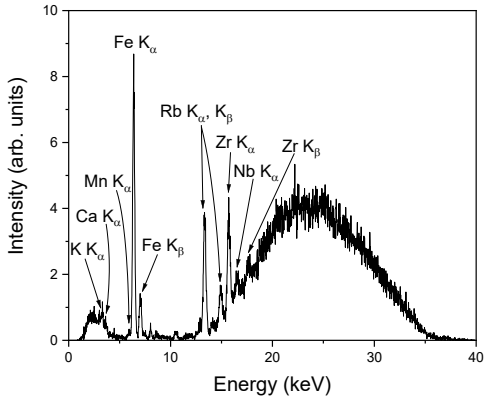

Fig. 2. Representative XRF spectra recorded on the Lipari pumice natural stone, in the energy range between 0 and 40 keV.

XRF analysis identified major elements including Fe, and trace elements such as K, Mn, Ca, Rb, Zr, and Nb, reflecting the sample's volcanic nature and consistency with intermediate-felsic products characteristic of the Aeolian Arc [16]. The prominent K peak in the XRF spectrum aligns with high ^{40}K activity and is likely due to the presence of K-bearing phases (e.g., sanidine or orthoclase). Furthermore, the presence of Rb may relate to magmatic differentiation processes, while High Field Strength Elements (HFSE) like Zr and Nb are crucial for tracing magma sources and evolution [17], often residing in accessory minerals. In detail, the presence of accessory phases containing Zr and Nb (e.g. zircon and niobates) likely explains the significant ^{232}Th and ^{226}Ra activities, especially due to their known ability to incorporate Th and U. Additionally, Fe and Mn may be associated with oxides and minor ferromagnesian phases contributing to the overall radioactivity.

Figure 3 shows the most representative XRD diffractogram for the investigated sample.

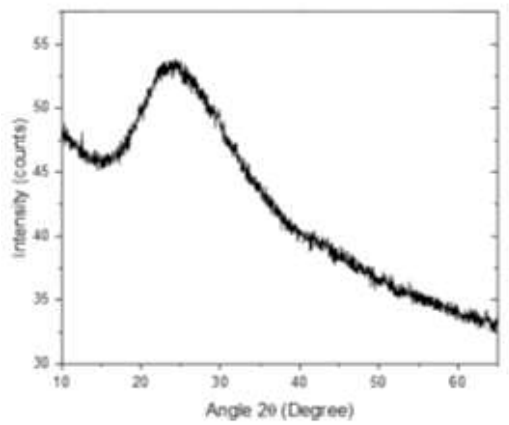

Fig. 3. XRD spectrum of the Lipari pumice sample.

It is worth noting that XRD analysis highlights the material's glassy nature. In detail, the low intensity of any discernible XRD peaks and the presence of a broad amorphous halo between 20° and 30° 2θ corroborate the dominance of volcanic glass and suggest that accessory phases are present in concentrations below the instrument's detection limit. In particular, the absence of sharp crystalline peaks and only weak, diffuse signals indicate a minor crystalline content, consistent with rapid post-eruptive cooling. In fact, rapid quenching can produce a matrix dominated by glass, as seen by XRD, while still preserving the melt's original elemental composition.

In the light of the above, the discrepancy between the elemental composition detected via XRF (see Figure 2) and the apparent absence or mismatch of corresponding crystalline phases in the XRD diffractogram (see Figure 3) can be attributed to the predominantly amorphous nature of the sample. Therefore, the elements detected through XRF analysis (i.e. K, Zr and Nb) and responsible for the observed radioactivity content are likely hosted within cryptocrystalline accessory phases or incorporated in solid solution within the glassy matrix, as commonly reported in silicic pyroclastic products [18]. Finally, the integration of radiological information, revealing significant ^{232}Th, ^{226}Ra and ^{40}K activity concentrations potentially hosted by accessory phases containing K, Zr and Nb, alongside elemental and mineralogical analyses, points to the Lipari pumice sample represents a typical product of evolved calc-alkaline magmatism within a subduction-related setting [19].

IV. CONCLUSIONS

Natural radioactivity content, elemental and mineralogical composition of a pumice rock sample from Lipari (Sicily, Southern Italy) were, for the first time, investigated and reported as a case study. The absorbed gamma dose rate (D), the Annual Effective Dose Equivalent (AEDE), the activity concentration index (I_γ) and the alpha index (I_α) were calculated to evaluate the potential radiological hazard associated with prolonged radiation exposure from the analyzed rock, particularly considering its widespread use as a building material both within and beyond the investigated area. In particular, all the assessed radiological hazard indices exceeded the threshold values set by Italian Legislation, with the exception of the alpha index (I_α), which was below but close to unity. However, this outcome reflects an extremely conservative exposure scenario, and highlights the need for a more detailed dose assessment, particularly for use in dwellings and buildings with a high occupancy factor.

Finally, XRF and XRD measurements were carried out to properly link the radioactive content to the elemental and mineralogical composition. Specifically, although mineralogical characterization revealed a predominantly glassy matrix, XRF analysis provided more detailed informations, offering valuable insight into the factors contributing to the observed radioactivity content. In particular, the high ^{40}K activity concentration could be consistent with the presence of K-rich feldspars such as sanidine and orthoclase, while the elevated activity concentrations of ^{232}Th and ^{226}Ra are likely associated with accessory Zr- and Nb-bearing phases, such as zircon and niobates, given their characteristic ability to incorporate Th and U.

REFERENCES

[1] D. Shahbazi-Gahrouei, et al., "A review on natural background radiation." Adv. Biomed. Res. vol. 2 (2013) 65.

[2] F. Caridi, et al., "Radon exhalation rate, radioactivity content, and mineralogy assessment of significant historical and artistic interest construction materials." Appl. Sci. vol. 14 (2024) 11359.

[3] G. Amato, et al., "La pomice per il confezionamento di calcestruzzi leggeri strutturali: Meccanica dei materiali e delle strutture." (2011).

[4] J. Monnet, "Soil and Rock Sampling Methods." John Wiley & Sons, Inc., Hoboken, NJ, USA (2015).

[5] F. Caridi, et al., "Multivariate statistics, radioactivity and radiological hazard evaluation in marine sediments of selected areas from Sicily, southern Italy." J. Mar. Sci. Eng. vol. 13 (2025) 769.

[6] F. Caridi, et al., "Evaluation of the radiological and chemical risk for public health from flour sample investigation." Applied Sciences 11.8 (2021): 3646.

[7] EC, "Radiation Protection 112: Radiological protection principles concerning the natural radioactivity of building materials." Eur. Comm., Brussels, Belgium (1999) 1–16.

[8] United Nations Scientific Committee on the Effects of Atomic Radiation (UNSCEAR), "Sources and effects of ionizing radiation (Report to the General Assembly)." United Nations, New York (2000).

[9] Italian D.Lgs. 101/20, "Legislation." (2020). Available online: https://www.normativa.it/ (accessed on 18 April 2025).
[10] NEA-OECD, "Exposure to radiation from natural radioactivity in building materials." NEA Group of Experts OECD (1979).
[11] S. Righi and L. Bruzzi, "Natural radioactivity and radon exhalation in building materials used in Italian dwellings." J. Environ. Radioact. vol. 88 (2006) 158–170.
[12] F. Caridi, et al., "Radioactivity content in construction materials of assets of particular historical-artistic interest." *Proc. IMEKO TC4 Int. Conf. Metrol. Archaeol. Cult. Herit.*, vol. 2023 (2023) 19–21.
[13] M. Degerlier, "Assessment of natural radioactivity and radiation hazard in volcanic tuff stones used as building and decoration materials in the Cappadocia region, Turkey." *Radioprotection*, vol. 48 (2013) 215–229.
[14] F. Caridi, et al., "Evaluation of radioactivity and heavy metals content in a basalt aggregate for concrete from Sicily, southern Italy: A case study." Appl. Sci. vol. 13 (2023) 4804.
[15] EC (2013) Council Directive 2013/59/Euratom of 5 December 2013 laying down basic safety standards for protection against the dangers arising from exposure to ionising radiation, and repealing Directives 89/618/Euratom, 90/641/Euratom, 96/29/Euratom, 97/43/Euratom and 2003/122/Euratom
[16] A. Peccerillo, "Plio-Quaternary volcanism in Italy." Springer (2005).
[17] H. Rollinson, "Using geochemical data: Evaluation, presentation, interpretation." Longman (1993).
[18] P. W. O. Hoskin, "Trace-element composition of hydrothermal zircon and the alteration of Hadean zircon from the Jack Hills, Australia." Geochim. Cosmochim. Acta vol. 69 (2005) 637–648.
[19] R. M. Ellam, "The transition from calc-alkaline to potassic volcanism in the Aeolian Islands, southern Italy." Open Univ. (1987).